EVALUATION ON BIOLOGICAL TISSUE EQUIVALENT AGAR-BASED SOLID PHANTOMS UP TO 10 GHZ – AIMING AT MEASUREMENT OF CHARACTERISTICS OF ANTENNA FOR UWB COMMUNICATIONS –

Takuya Takimoto[†], Teruo Onishi[††,†], Kazuyuki Saito[†††], Masaharu Takahashi[†††], Shinji Uebayashi[††], and Koichi Ito[†††]
† Graduate School of Science and Technology, Chiba University
1-33 Yayoi-cho, Inage-ku, Chiba 263-8522, Japan
†† NTT DoCoMo, Inc., 3-5 Hikarinooka, Yokosuka 239-8536, Japan
††† Research Center for Frontier Medical Engineering, Chiba University
1-33 Yayoi-cho, Inage-ku, Chiba 263-8522, Japan
E-mail: takimoto@graduate.chiba-u.jp

1. Introduction

Recently, frequencies used by wireless LAN devices that are higher than the ones used by the present cellular systems have become popular and the UWB (Ultra Wide Band) [1] communication systems, which employ a very wide frequency range from 3.1 GHz to 10.6 GHz, are currently under development. The UWB systems enable a high speed communication at short distance, and are expected to be used in the vicinity of the human body. Up to now, many studies on the interaction between EM (Electromagnetic) waves and human body focusing on the present cellular systems have been conducted [2], [3]. It is also important to evaluate the interaction in the higher and/or broadband frequency range. From this point of view, biological tissue-equivalent phantoms applied to these frequencies are required.

The authors have already developed biological tissue-equivalent agar-based solid phantoms which reproduce the electrical properties of the human body for broadband applications [4], [5]. Since the phantoms have broadband characteristics, we can measure the characteristics of the antenna close to the human body without changing the phantom at each frequency. In other word, a unique phantom can be used for the measurement of characteristics of broadband antennas.

In this paper, the feasibility to evaluate of the characteristic of the antenna is examined by using the developed phantoms that have broadband characteristics. First, we adjust the composition of the phantom for the frequency range from 2 GHz to 10 GHz and compare its electrical properties with the target values. Next, some characteristics of the antenna close to this phantom (such as input impedance, radiation pattern, etc) are analyzed by numerical calculations. Then, we compare the calculated results obtained with this phantom to the target value and evaluate the difference between these results. Moreover, the local SAR (Specific Absorption Rate) inside the phantom is also investigated.

2. Electrical constants of the biological tissue equivalent solid phantom

In this paper, we choose the frequency range from 2 GHz to 10 GHz with 1 GHz step. Moreover, 2.45 GHz, which is one of the ISM (Industrial, Scientific and Medical) frequencies, is also considered. The target values are set to 2/3-muscle equivalent tissues called the 2/3-muscle model, which corresponds the electrical constants of muscle equivalent tissues [6] times 2/3. Table 1 shows the composition of the 2/3-muscle equivalent solid phantom used in this research. The measured electrical constants of the 2/3-muscle model are shown in Fig. 1. Error-bars indicate a ±5% divergence from the target values. Moreover, differences in the electrical constants between the target values and the measurements at each frequency are shown in Fig. 2.

Table 1 Composition of the 2/3-muscle model. (A batch is approximately 4,500 g.)

Material	Amount [g]
Deionized Water	3,375.0
Agar	104.6
Polyethylene Powder	1,012.6
Sodium Chloride	7.0
TX-151	30.1
Dehydroacetic Acid Sodium Salt	2.0

ISBN: 89-86522-78-0 94460©KEES

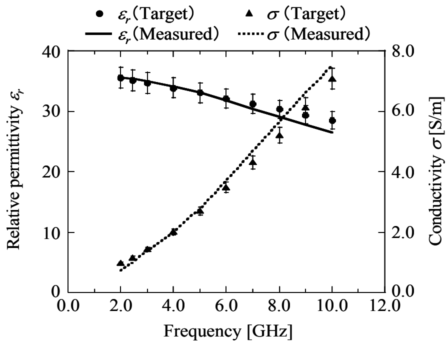

Fig. 1 Measured electrical constants of 2/3-muscle model versus frequency.

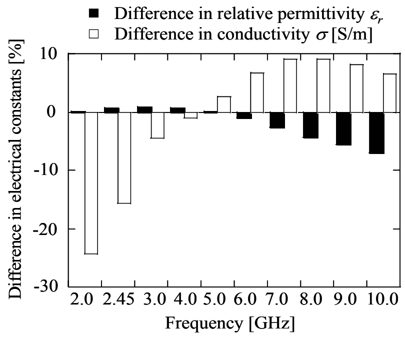

Fig. 2 Differences in the electrical constants of a 2/3-muscle model between measurements and targets.

From Fig. 1, it is clear that all the measured relative permittivities are within ±5% of the target values except at 9 GHz and 10 GHz. However, from Fig. 2 the measured conductivities are within ±5% only from 3 to 6 GHz. If a variation of ±10% from the target value is allowed, electrical constants for 3-10 GHz frequency range are within this range. In addition, it is also possible to adjust the electrical constants exactly for a desired frequency by changing the amount of polyethylene powder and sodium chloride.

3. Calculation model

In this paper, the effects due to the variation of the electrical constants of the phantom on the antenna characteristics are described. Figure 3 shows the numerical calculation model. The half-wavelength dipole antenna is employed as a radiator of electromagnetic energy. It is noted that the length of the antenna is adjusted to $0.47\lambda_0$ at each frequency, where λ_0 is the wavelength in free space. The size of the phantom is 100 mm × 200 mm × 200 mm. The location of the antenna is fixed at 10 mm away from the phantom surface. The origin of the coordinate directly faces the antennas feeding point and is located on the surface of the phantom.

The FD-TD method is used for numerical calculations. In the FD-TD calculations, graded meshes are employed to reduce the computational time and required memory. It is noted that the maximum cell size does not exceed $1/10\lambda_g$, where λ_g is the wavelength in the phantom. The absorbing boundary condition is the perfectly matched layer (PML) (eight layers), and the input signal at the feed point of the antenna is a sine wave. The number of iterations is ten periods at each frequency.

The input impedance (S_{11}), radiation efficiency, and radiation patterns of the half-wavelength dipole antenna are evaluated at each frequency. In addition, the local SARs are also calculated.

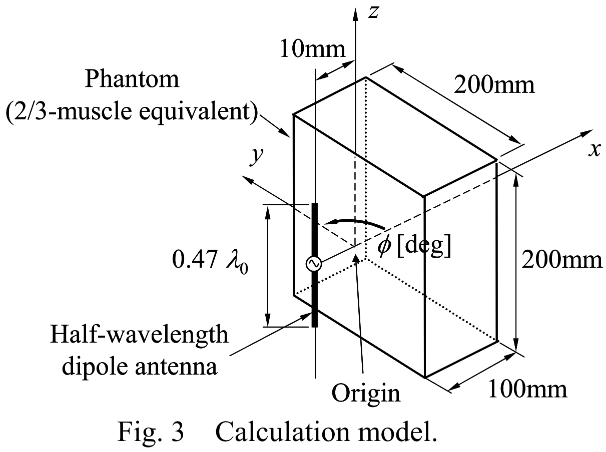

Fig. 3 Calculation model.

4. Results

Figure 4 shows the calculated input impedances (S_{11}) of the dipole antennas. The "target" and the "empirical" correspond to the calculated results based on the target and measured electrical constants of the 2/3 muscle equivalent phantom, respectively. As it can be seen from Fig. 4, although the measured electrical constants of the phantom diverge from the target values at upper and lower frequencies (Fig. 2), the differences of S_{11} between them are negligible over the whole frequency range.

For example at 2 GHz, the difference of S_{11} is about 3% although the difference between both target and measured conductivity is -24%. Additionally, it can be expected that this difference does not generally influence the characteristic of the antenna in far field as much as 2 GHz. Moreover, it was clarified from this graph that S_{11} of the dipole antenna in the near field is not influenced either.

Figure 5 shows the calculated radiation efficiency of the dipole antennas. From this graph, it is also clear that the efficiencies based on the empirical values are almost the same as the target ones. Moreover, the radiation efficiency is improved with an increase in the frequency. This is because the distance between the antennas and the phantom is fixed to 10 mm. However, the distance normalized to each wavelength varies with the frequency. As the location of the antenna is equivalently moved away from the phantom at higher frequency, the EM wave absorbed by the human body decreases. As a result, the radiation efficiency increases.

Figure 6 shows the calculated radiation patterns of the dipole antennas in the horizontal plane. These results are shown only from 0° to 180°, because the calculation model has a symmetrical structure. As can be seen from Fig. 6 (b) and (c), it is clear that the patterns based on the empirical value are almost the same as the results based on target value at 5 GHz and 10 GHz. However, as can be seen from Fig. 6 (a), we confirmed a difference of approximately 10 dB in the direction of the back lobe at 2 GHz. At 2 GHz, it is considered that the radiation pattern changed because of the large amount of difference for the conductivity of the phantom as shown in Fig. 2. However, both the target and the empirical radiation patterns in the direction of main lobe at all frequencies excellently match.

Figure 7 shows the calculated results of SARs. From Fig. 7 (a), it can be confirmed for the peak SARs that the difference between the targets and the empirical values are from -10 to +22% (compared to the targets). Therefore, it was clarified for the peak SAR that a change occurs proportionally to the amount of the difference in the electrical constants. Moreover, as can be seen from Fig. 7 (b) and (c), the change for 1 and 10 g averaged SARs, which depend on the difference of the electrical constants, increases at the low frequency.

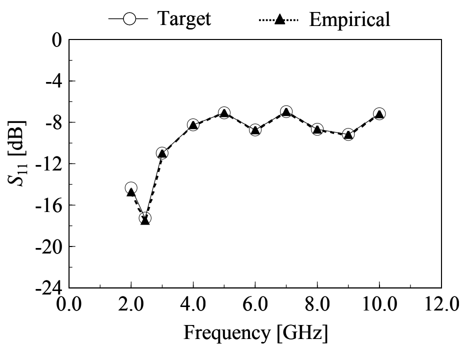

Fig. 4 Calculated input impedances (S_{11}) of the antenna.

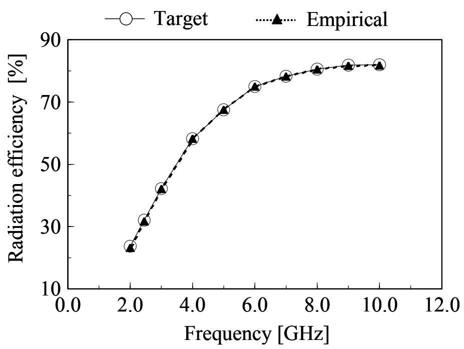

Fig. 5 Calculated radiation efficiency of the antenna.

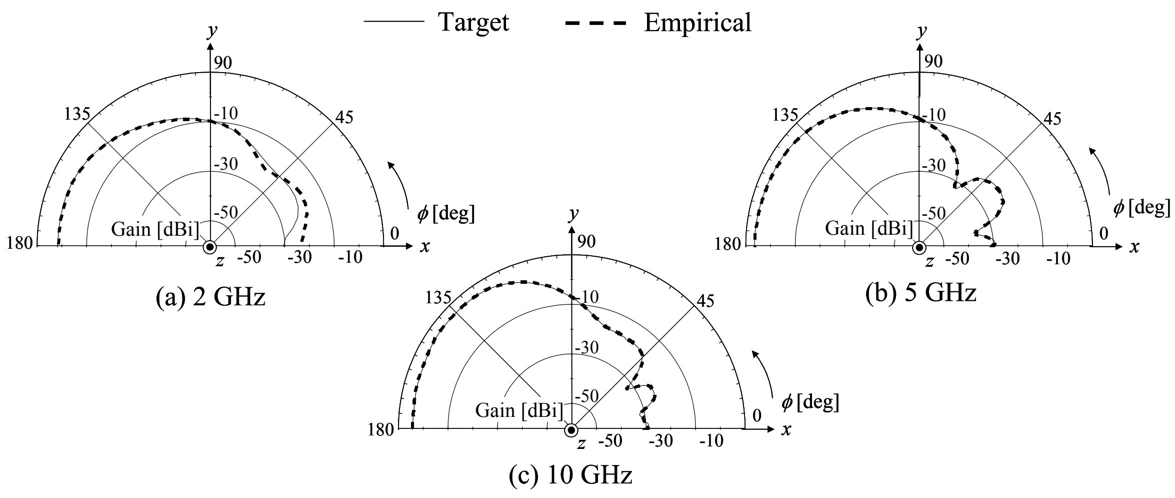

Fig. 6 Calculated radiation patterns of the antenna.

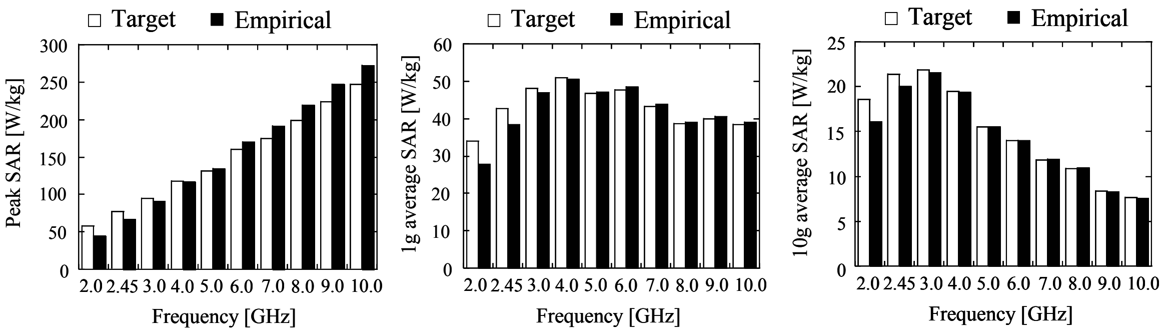

(a) Peak SAR (b) 1 g average SAR (c) 10 g average SAR

Fig. 7 Calculated maximum values of local SAR at each frequency.

5. Conclusions

In this paper, the evaluations of the characteristics of a biological tissue-equivalent agar-based solid phantom in the range of 2-10 GHz were described. It is confirmed that this phantom can be applied to a high and wide frequency range up to 10 GHz. In these frequencies, the maximum difference of the electrical constants of the phantom is less than -24% at 2 GHz. In order to evaluate the effects due to the difference between target and measured electrical constants of the phantom, the FD-TD calculations were employed. In addition, the local SARs inside the phantom was also clarified. As a result, the difference of the electrical constants of phantom does not influence the input impedance (S_{11}), radiation efficiency, and radiation patterns of a half-wavelength dipole antenna so much. Moreover, the local peak SAR increases in proportion to the amount of the difference of the electrical constants, and the change in the 1 and 10 g averaged SARs, which depend on the difference of the electrical constants, increases at low frequency.

From these results, we confirmed that the tissue-equivalent agar-based solid phantom, which is developed by us, can be used to evaluate antenna characteristics up to 10 GHz.

Acknowledgment

The authors are grateful to Dr. Hanazawa, Dr. Wake, and Dr. Watanabe of the National Institute of Information and Communication Technology (NICT), Japan, for their supports on the measurements of electrical constants of the phantom.

References

[1] FCC Part 15 “Radio frequency devices,” FCC, USA, 2003.

[2] M. A. Jensen and Y. Rahmat-Samii, “EM interaction of handset antennas and a human in personal communications,” *Proc. IEEE*, vol. 83, no. 1, pp. 7-17, Jan. 1995.

[3] S. Watanabe, M. Taki, and T. Nojima, “Effects of the interaction between a human head and a hand-held portable radio on the antenna input impedance,” *Trans. IEICE* (B-II), vol. J79-B-II, no. 9, pp. 557-565, Sep. 1996 (in Japanese).

[4] R. Ishido, T. Onishi, K. Saito, S. Uebayashi, and K. Ito, “A study in the solid phantom for 3-6 GHz and evaluation of SAR distribution based on the thermographic method,” *Proc. EMC’04 Sendai*, 3B3-2, Sendai, Japan, Jun. 2004.

[5] T. Onishi, T. Takimoto, K. Saito, S. Uebayashi, M. Takahashi, and K. Ito, “Biological tissue-equivalent agar-based solid phantoms with wide band characterintics up to 10 GHz,” *Proc. 2005 BioEM Meeting*, Dublin, Ireland, Jun. 2005 (to be presented).

[6] S. Gabriel, R.W. Lau, and C. Gabriel, “The dielectric properties of biological tissues: II. Measurements in the frequency range 10 Hz to 20 GHz,” *Phys. Med . Biol.* 41, pp. 2251-2269, Apr. 1996.